Conf-830805--24

Finite-Element Blunt-Crack Propagation -- A Modified J-Integral Approach

Y. C. Pan, A. H. Marchertas and J. M. Kennedy
Engineering Mechanics Program
Reactor Analysis and Safety Division
Argonne National Laboratory
Argonne, Illinois 60439, U.S.A.

CONF-830805--24

DE83 010579

ARGONNE NATIONAL LABORATORY

DISCLAIMER

Abstract

In assessing the safety of a liquid metal fast breeder reactor (LMFBR), a major concern is the behavior of concrete structures subjected to high temperatures. The potential of concrete cracking is an important parameter which could significantly influence the safety assessment of thermally attacked concrete. A new modified J-integral approach for the blunt crack model has been derived to provide a general procedure to accurately predict the direction of crack growth. This formulation has been incorporated into the coupled heat transfer-stress analysis finite element code TEMP-STRESS. A description of the formulation is presented in this paper. Results for the problems of a Mode I and mixed mode crack in a plate using regular and slanted meshes subjected to uniaxial and shear loading are presented. Energy release rates calculated by the J-integral agree well with the theoretical predictions for a Mode I crack problem with different mesh representations. However, engineering judgment and great care must be exercised in grid discretization for a mixed mode crack problem to capture the shear singularity.

1. Introduction

The effects of high temperature on the integrity of concrete structures is of vital concern in the design of a safe and reliable LMFBR plant. Such effects can become manifest by exposure to high temperatures in the reactor cavity under cavity cooling system malfunctions or core melt accidents and spillage of large quantities of hot reactor coolant onto steel-lined concrete structures. An important parameter which must be addressed in the safety assessment of concrete structures is the potential of cracking due to this thermal attack. Cracking, in general, reduces the integrity of the structure plus provides pathways for hostile attack of the coolant upon the concrete. The prediction of crack initiation and crack propagation in concrete is, therefore, very important in the safety assessment of a LMFBR.

Concrete cracking in finite element analysis can be modeled as a blunt crack where the element represents the crack. The element has uniform crack distribution throughout its area. In contrast to the sharp crack model where the crack loses all its load carrying capacity, the blunt crack model allows the cracked element to transmit stress parallel to the crack direction. Bazant and Cedolin [1] developed a blunt crack model based on the energy release rate and the effective strength concepts. This model is insensitive to the element size. Difficulties were encountered in implementing their approach into a general purpose finite element code due to the absence of a general procedure to accurately predict the direction of crack growth [2]. A procedure based on a modified J-integral has been developed to overcome this difficulty.

This modified J-integral formulation has been incorporated into the general purpose nonlinear finite element code TEMP-STRESS [3]. The basic framework of TEMP-STRESS has been taken from the STRAW computer code [4,5,6]. TEMP-STRESS is a weakly coupled heat transfer-stress analysis code. The code uses an explicit integration scheme, coupled with dynamic relaxation to solve problems of structures subjected to high temperatures. The J-integral procedure and numerical computations are described in the following sections.

2. J-Integral for the Blunt Crack Model

A blunt crack of length a is assumed to advance a small amount Δa in an arbitrary direction $\bar{x}$. After the crack advances, the material in the incremental volume ΔV is assumed to retain only its capability to transmit the stress $\sigma_{\bar{x}}$ parallel to the crack direction. The energy change associated with the crack advancement in this case was shown in Ref. [1] as

$$\Delta U = -\frac{1}{2}\int_{\Delta V}(\overset{o}{\sigma}_{ij}\overset{o}{\varepsilon}_{ij} - \sigma_{\bar{x}}\varepsilon_{\bar{x}})dV + \frac{1}{2}\int_{\Delta S}\Delta T_i(u_i - \overset{o}{u}_i)dS \ , \qquad (1)$$

where ΔV is the volume change, ΔS is the change in surface area, σ_{ij} is the stress, ε_{ij} is the strain, u_i is the displacement, ΔT_i is the change in surface traction and the superscript, o, denotes the original state before the crack advances.

If Δa is assumed to be infinitesimally small as in the J-integral approach [7], the second integral in Eq. (1) reduces to zero and the following expression can be obtained for the energy release rate at the crack tip:

$$G = -\frac{dU}{da} = \frac{1}{2}\int_{tip} (\sigma^0_{ij}\varepsilon^0_{ij} - \sigma_{\bar{x}}\varepsilon_{\bar{x}})dy \ , \tag{2}$$

where y is normal to the crack direction $\bar{x}$. It is noted that the first term in Eq. (2) is equal to the well known J-integral and the second term accounts for the remaining load carrying capacity of the cracked element. Therefore, the first term in Eq. (2) can be evaluated by integrating the following equation around an arbitrary loop Γ surrounding the crack tip

$$J_{\bar{x}} = \int_{\Gamma} \left(W^0 - T^0 \cdot \frac{\partial u^0}{\partial \bar{x}}\right) d\bar{y} \ , \tag{3}$$

where

$$W^0 = \frac{1}{2}\sigma^0_{ij}\varepsilon^0_{ij} \ .$$

In deriving Eq. (2), it is assumed that the shape of the crack tip remains the same before and after the crack advances. Hence, the second term in Eq. (2) is only a constant. G and J are related by

$$G = k \cdot J \ . \tag{4}$$

Although the constant k can be obtained by numerically evaluating G and J, its determination is not necessary since J can be used directly in the crack propagation criterion.

According to J-integral theory [7,8], the crack will propagate in the direction where the J-integral value is a maximum and the crack propagates if the J-integral reaches a critical value. It is also pointed out in Ref. [9] that the J value should be calculated by using the elastic solution of a deflected crack, having a main branch and a propagating branch. If we assume that the distribution of the elastic field of a blunt crack is similar to that of a sharp crack, then the crack propagation directions predicted by the sharp crack model and the blunt crack model would be the same.

The solution for a deflected crack would make the numerical programming extremely difficult. However, the energy release rate associated with a kinked crack was obtained in Ref. [9]:

$$J = \frac{4}{E}\left(\frac{1}{3 + \cos^2\theta}\right)^2 \left(\frac{1 - \theta/\pi}{1 + \theta/\pi}\right)^{\theta/\pi} [(1 + 3\cos^2\theta)K_I^2$$

$$+ 8\sin\theta\cos\theta K_I K_{II} + (9 - 5\cos^2\theta)K_{II}^2] \ , \tag{5}$$

where E is the Young's modulus, θ is the propagation angle, $\pi = 3.14159$, K_I and K_{II} are the stress intensity factors for Mode I and Mode II cracks. K_I and K_{II} are related to the J-integral based on the original crack configuration and the global Cartesian coordinates with x parallel to the crack direction by the relation

$$J_x = \beta \cdot (K_1^2 + K_2^2) \ ,$$

$$J_y = \beta \cdot (2K_1K_2) , \tag{6}$$

where $\beta = \frac{1}{E}$ for plane stress condition and $\beta = (1 - \nu^2)/E$ for plane strain condition. Hence we can now obtain the J value and the crack propagation angle by evaluating J_x and J_y. In the case where Mode I deformation dominates, the crack propagation direction will be small. Eq. (5) reduces to

$$J = J_x \cos\theta + J_y \sin\theta \tag{7}$$

and the propagation angle becomes

$$\theta = \tan^{-1}\left(\frac{J_y}{J_x}\right).$$

In the J-integral evaluation, it is noted that the surface traction vanishes on the blunt crack surface just as on the sharp crack surface. Therefore, the numerical integration for the blunt crack model is similar to that for the sharp crack model. The second term in Eq. (3) always vanishes on the top and bottom surfaces of the crack, whereas, the first term vanishes only under the following conditions:

(1) if $d\bar{y} = 0$, namely, the crack propagates in the same direction as before,

(2) if W on the top surface is the same as that on the bottom surface. This occurs in both symmetric and skew symmetric conditions.

Hence the J-integral can be evaluated on an arbitrary loop which starts and ends on the opposite sides of the crack surfaces under these conditions.

In the finite element discretization, an additional complication enters if the crack direction is not the same as the mesh direction. In that case, the crack has to be represented by a zig-zag band. Once the direction is calculated, the crack is assumed to advance to the element which introduces the least amount of accumulated error as defined by

$$\theta^N_{err} = \sum_{i=1}^{N} (\theta^i - \theta^i_J) , \tag{8}$$

where θ^i_J is the cracking angle calculated by the J-integral approach, θ^i is the angle subtended by the reference axis and a line joining the centroids of the i^{th} and the last cracked elements. The i^{th} element is adjacent to the last cracked element. The minimization of error in Eq. (8) then forces the crack to take a zig-zag path which is close to the correct cracking direction. After the prospective crack element and the crack direction are determined, the crack is assumed to propagate when the energy release rate reaches a critical value.

The above described approach has been incorporated into the general purpose finite element code TEMP-STRESS [3]. A Gaussian integration scheme is used for the J-integral. The program is set up so that the user can select the integration path and the number of Gaussian

integration points. The subroutines are fully integrated into the TEMP-STRESS code so that the time history of the J-values can be plotted. The application of these procedures to the plane stress problem of a cracked plate using quadrilateral elements with one point integration and elastic hourglass control [10] is described in the following sections.

3. Numerical Calculations for the J-Integrals

Mode I Crack

The plane stress problem of a Mode I crack in a plate subjected to uniaxial loading was first studied. Two different types of meshes as shown in Figs. 1(a) and 1(b) are used. The solid line in Fig. 1(b) indicates the coarse slanted mesh whereas the dotted line indicates the fine mesh. The integration loops for the J-integrals are shown as the bold lines. All computations were performed for $E = 2.193\ MN/m^2$, $\nu = 0.2$, $b = 0.24$ m, $h = 0.26$ m and $J_c = 0.0236$ MN/m. The applied stress is kept at $5000\ N/m^2$ for all runs.

From mesh 1(a), it can be readily seen that the J-integrals over the top and bottom surfaces of the crack vanished. For mesh 1(b) this is not so apparent. However, one can argue that if the straight crack shown in Fig. 1(a) can be represented by the zig-zag crack band shown in Fig. 1(b), then the elastic fields associated with the two models should be the same and similar integration loops should yield the same results. Therefore, one would expect the J-integrals over the top and the bottom surface of the zig-zag band to cancel with each other and the error associated with an integration loop shown in Fig. 1(b) to be small. Different sizes of integration loops have been attempted, the numerical results indicate that the J-integral values are insensitive to the size of the integration loop and that the result for the zig-zag crack band is very close to that for the straight blunt crack.

For all numerical integrations performed using mesh 1(a), J_y is generally orders of magnitude smaller than J_x, resulting in a predicted crack angle nearly 0°. Hence, the crack advances in a straight line shown as the shaded area in Fig. 1(a). For mesh 1(b), J_y is generally at least an order of magnitude smaller than J_x, yielding a predicted crack angle of less than 5°. Therefore, the crack takes a zig-zag path as shown in Fig. 1(b) by applying Eq. (8) for choosing the cracking elements. The calculated load multiplier α, where $\alpha\sigma$ gives the critical stress for crack extension, is plotted in Fig. 2 (along with the theoretical predictions). In this figure, the length of the zig-zag crack band is taken as the projected length on the crack direction. It is noted that there is very good agreement between the numerical results and the theoretical predictions indicating that the J-integral approach can be used with the blunt crack model and that the zig-zag crack band can be used to represent the straight Mode I crack.

During this study, it is found that reasonable numerical results can be obtained without hourglass control. While an hourglass viscosity of 0.05 does not significantly affect the numerical results for the mesh shown in Fig. 1(a), the same hourglass viscosity causes the plate containing the zig-zag crack band to be much stiffer than the plate containing an equivalent straight crack. In general, an hourglass viscosity of 0.001 or less should be used in this type of problems.

Mixed Mode Crack

The plane stress problem of a center-cracked plate subjected to both normal and shear stresses was examined next. The material properties are the same as in the previous section. The applied normal and shear stresses are made equal so that the crack angle is expected to be -45 degrees [9].

Contrary to the good agreements between the theoretical values and the numerical calculations for Mode I crack, the calculated crack angle is -12° for the mesh shown in Fig. 3(a). In order to gain insight into the relationship among various parameters and the J-integrals, the effects of the hourglass viscosity, the size of the integration loop and the grid discretization are studied. It is found that hourglass control is essential for a mixed mode crack problem. An hourglass viscosity ranging from .001 to .005 is needed for the uncracked elements. The numerical results are relatively insensitive to the hourglass viscosity used in the cracked elements. J_x values are found to be insensitive to the size of the integration loop and the grid discretization, whereas, a small integration loop surrounding the adjacent elements to the crack tip seems to yield more reasonable J_y values. Mesh discretization is by far the most dominant factor in evaluating J_y. In the parametric study, the finite element mesh was first refined in the direction perpendicular to the crack surface as shown in Fig. 3(b). The results of the parametric study on mesh discretization are plotted in Fig. 4. It is noted that the change in crack angle is mainly related to the change in J_y. The observed behavior of the J-integral is consistent with the elastic field associated with the mixed mode crack. The normal stress ahead of the crack generally shows the singularity regardless of the grid discretization, whereas, the singularity of the shear stress shows up only after the mesh shown in Fig. 3(a) is refined. This indicates that the finite element mesh has to be chosen carefully to capture the elastic field associated with the Mode II crack.

It can be deduced from these studies that the numerical errors associated with a mixed mode crack could be large if a coarse finite element mesh is used. The error, however, would reduce as the crack tends toward Mode I as one would expect under a static loading condition. For demonstration purpose, the problem of uniaxially loaded plate containing a 23.6° slanted crack as shown in Fig. 5 is examined. The predicted zig-zag crack band is indicated by the shaded area. It is noted that the overall crack pattern looks reasonable even though the initial crack direction is quite different from the theoretical value.

4. Conclusions

The following conclusions can be made from this study:

(1) The J-integral approach works well with the blunt crack model.

(2) The approach works best for a Mode I crack where the numerical results are insensitive to the size of the integration loop and the grid discretization. Also, there is no hourglass problem.

(3) A zig-zag crack band can represent a straight Mode I crack.

(4) Engineering judgment and great care must be exercised in grid discretization for a mixed mode crack problem to capture the shear singularity. Proper hourglass viscosity and integration loop must be chosen. For the particular problem studied in this article, an hourglass viscosity of .001, a small integration loop and a fine grid at the crack tip several orders smaller than the crack length are needed to yield reasonable results for the incipient crack growth.

References

[1] Z. P. Bazant, and L. Cedolin, "Blunt Crack Propagation in Finite Element Analysis," Journal of the Engineering Mechanics Division, ASCE, Vol. 105, April 1979, pp. 297-315.

[2] A. H. Marchertas, R. F. Kulak, and Y. C. Pan, "Performance of the 'Blunt Crack' Approach Within a General Purpose Code," in Nonlinear Numerical Analysis of Reinforced Concrete, edited by L. E. Schwer, ASME Publication H00242, 1982.

[3] A. H. Marchertas and R. F. Kulak, "A Coupled Heat Conduction and Thermal Stress Formulation Using Explicit Integration," Argonne National Laboratory Report, ANL-82-47, June 1982.

[4] J. M. Kennedy, "Nonlinear Dynamic Response of Reactor-Case Subassemblies," ANL-8065 (Jan. 1974).

[5] D. F. Schoeberle, J. M. Kennedy, and T. B. Belytschko "Implicit Temporal Integration for Long-Duration Accidents in a Structural Response Code - STRAW," ANL-8136 (Oct. 1974).

[6] R. F. Kulak, T. B. Belytschko, J. M. Kennedy, and D. F. Schoeberle, "Finite Element Formulation for Thermal Stress Analysis of Thin Reactor Structures," Nuclear Engineering and Design, Vol. 49, 39-50 (1978).

[7] J. R. Rice, "A Path Independent Integral and the Approximate Analysis of Strain Concentration by Notches and Cracks," Journal of Applied Mechanics, Vol. 35, June 1968, pp. 379-386.

[8] H. C. Strifors, "A Generalized Force Measure of Conditions at Crack Tips," International Journal of Solids and Structures, Vol. 10, 1974, pp. 1389-1404.

[9] M. A. Hussain, S. L. Pu, and J. Underwood, "Strain Energy Release Rate for a Crack Under Combined Mode I and Mode II," in Fracture Analysis, ASTM STP 560, 1974, pp. 2-28.

[10] T. B. Belytschko and J. M. Kennedy, "Hourglass Control for Nonlinear Material Problems," Seventh Int. Conf. on SMiRT, Chicago, Illinois, August 1983, Paper L 13/1.

Fig. 1. (a) Blunt Crack Model in Rectangular Mesh.
(b) Blunt Crack Model in Slanted Mesh.

Fig. 2. Variation of the Load Multiplier Versus the Crack Length to Plate Thickness Ratio.

Fig. 3. (a) Mixed Mode Blunt Crack Model in a Coarse Mesh.
(b) Mixed Mode Blunt Crack Model in a Fine Mesh.

Fig. 4. Variation of the Incipient Crack Propagation Angle Versus the Grid Size to Crack Half Length Ratio.

Fig. 5. Mixed Mode Blunt Crack Propagation.

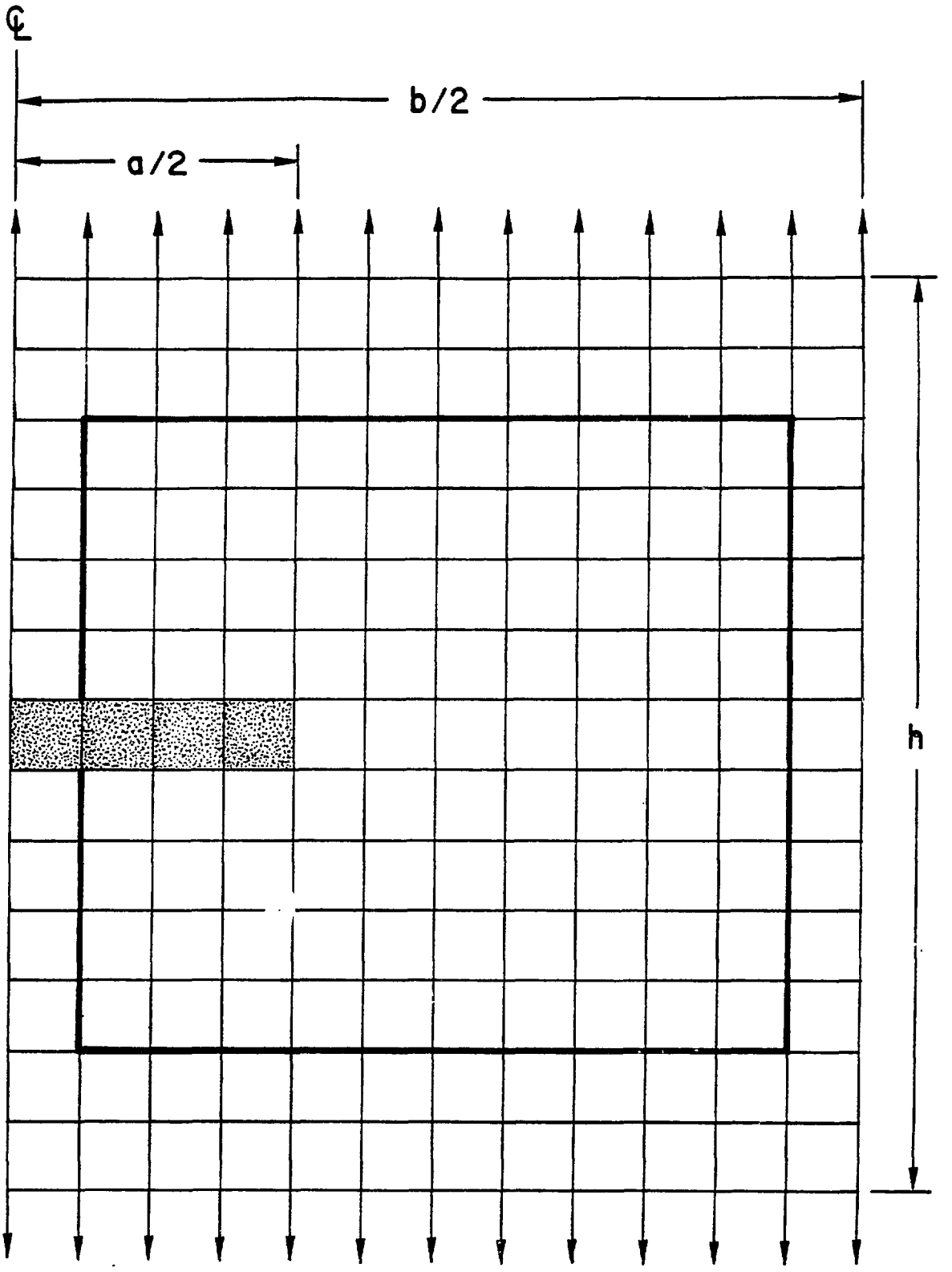

(a)

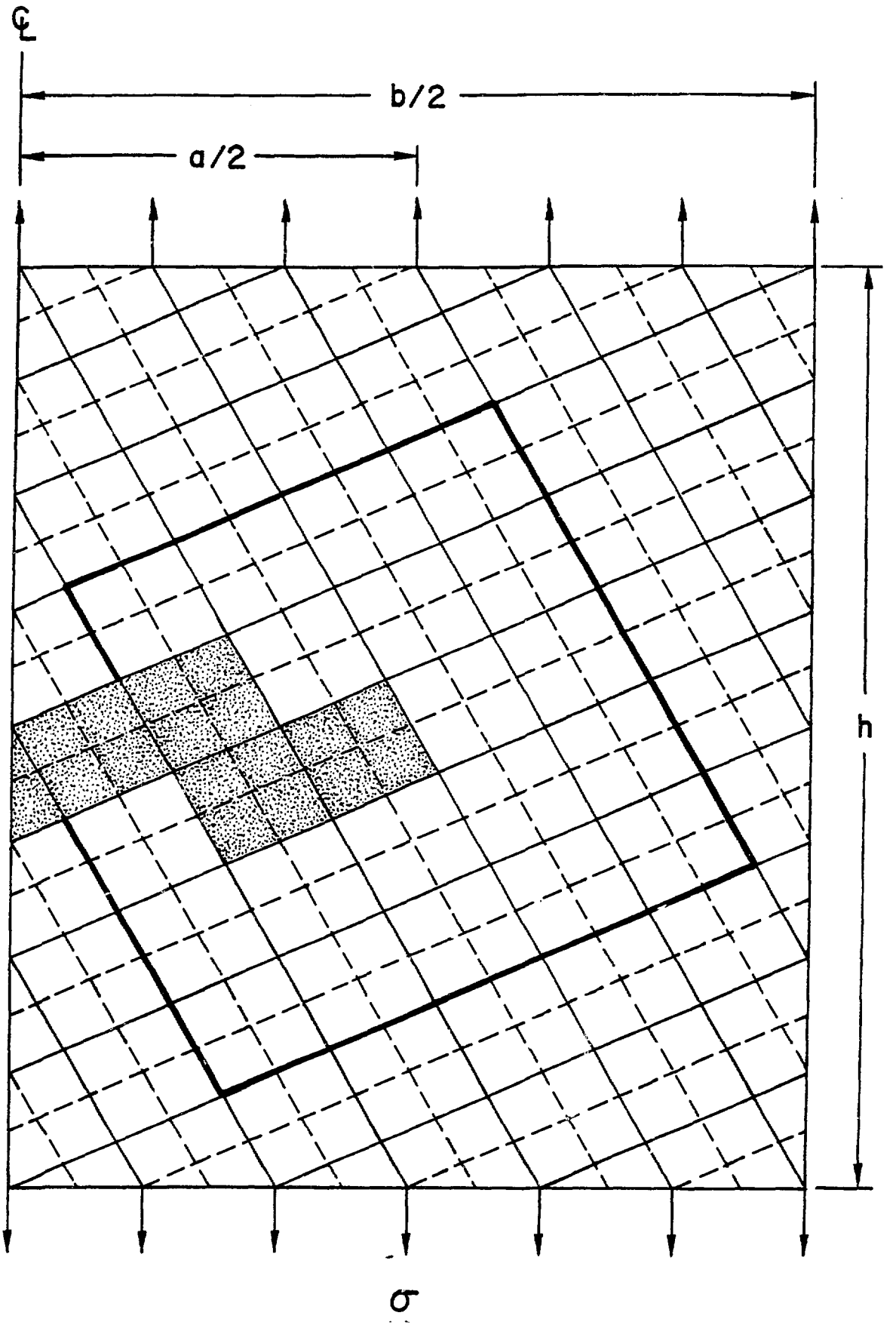

(b)

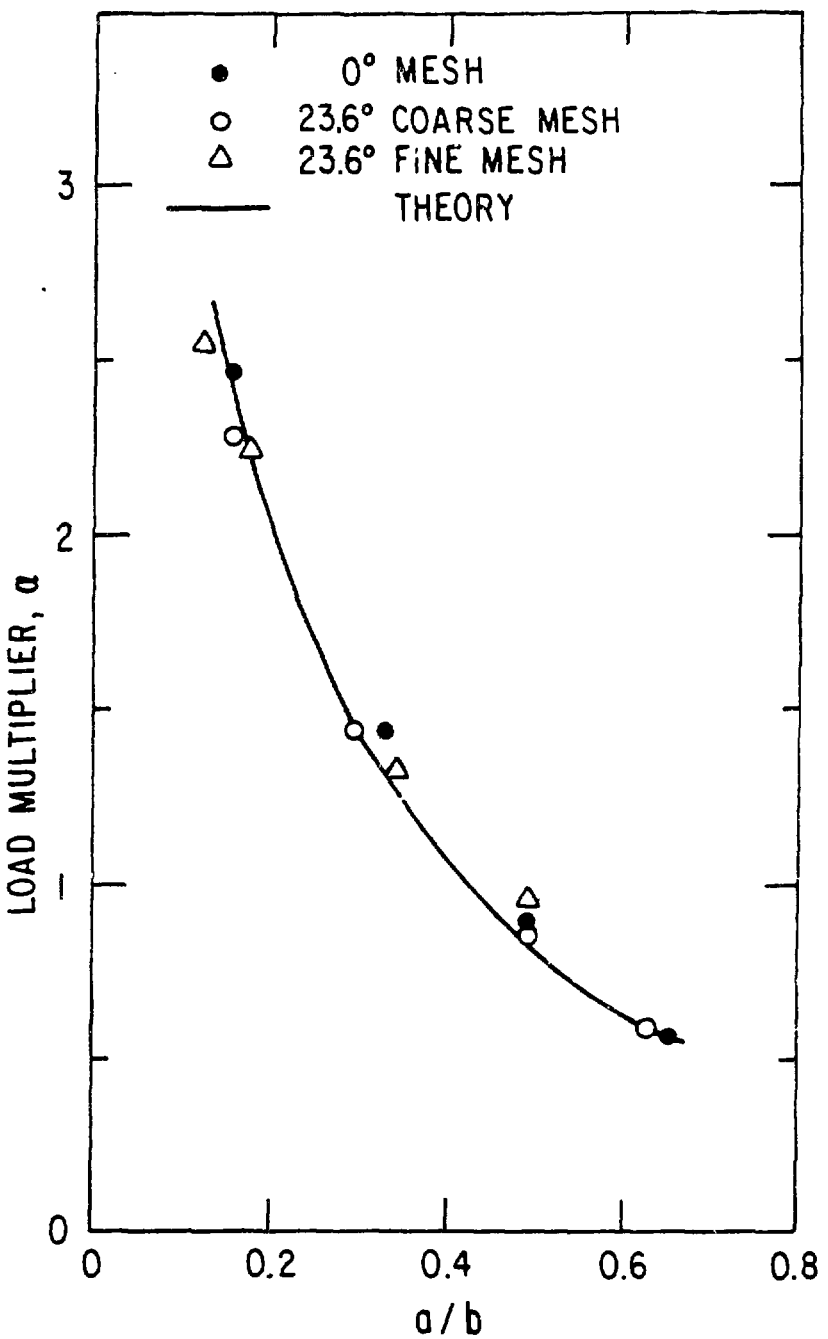
0° MESH
23.6° COARSE MESH
23.6° FINE MESH
THEORY
LOAD MULTIPLIER, α
0
1
2
3
0
0.2
0.4
0.6
0.8
a/b

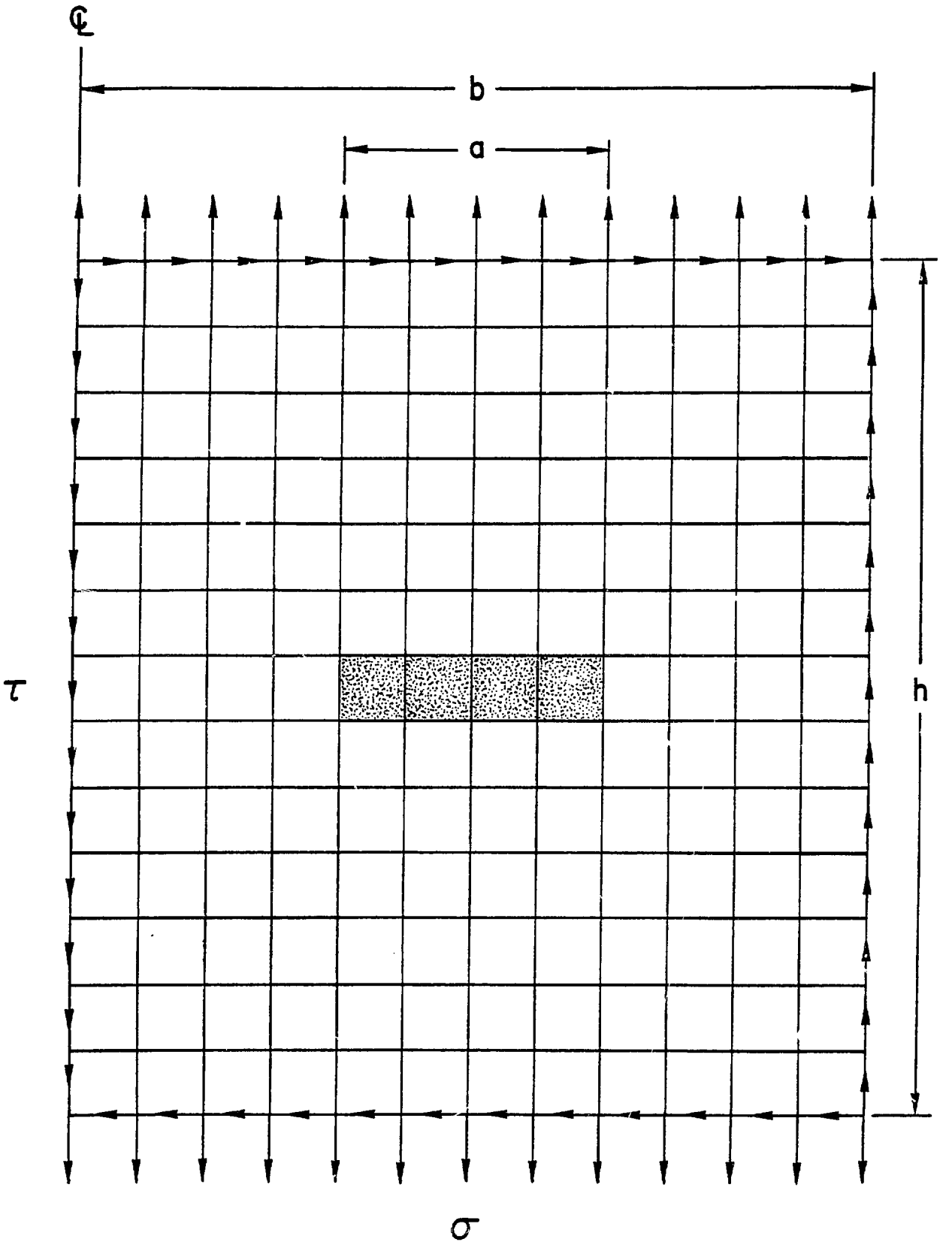

(a)

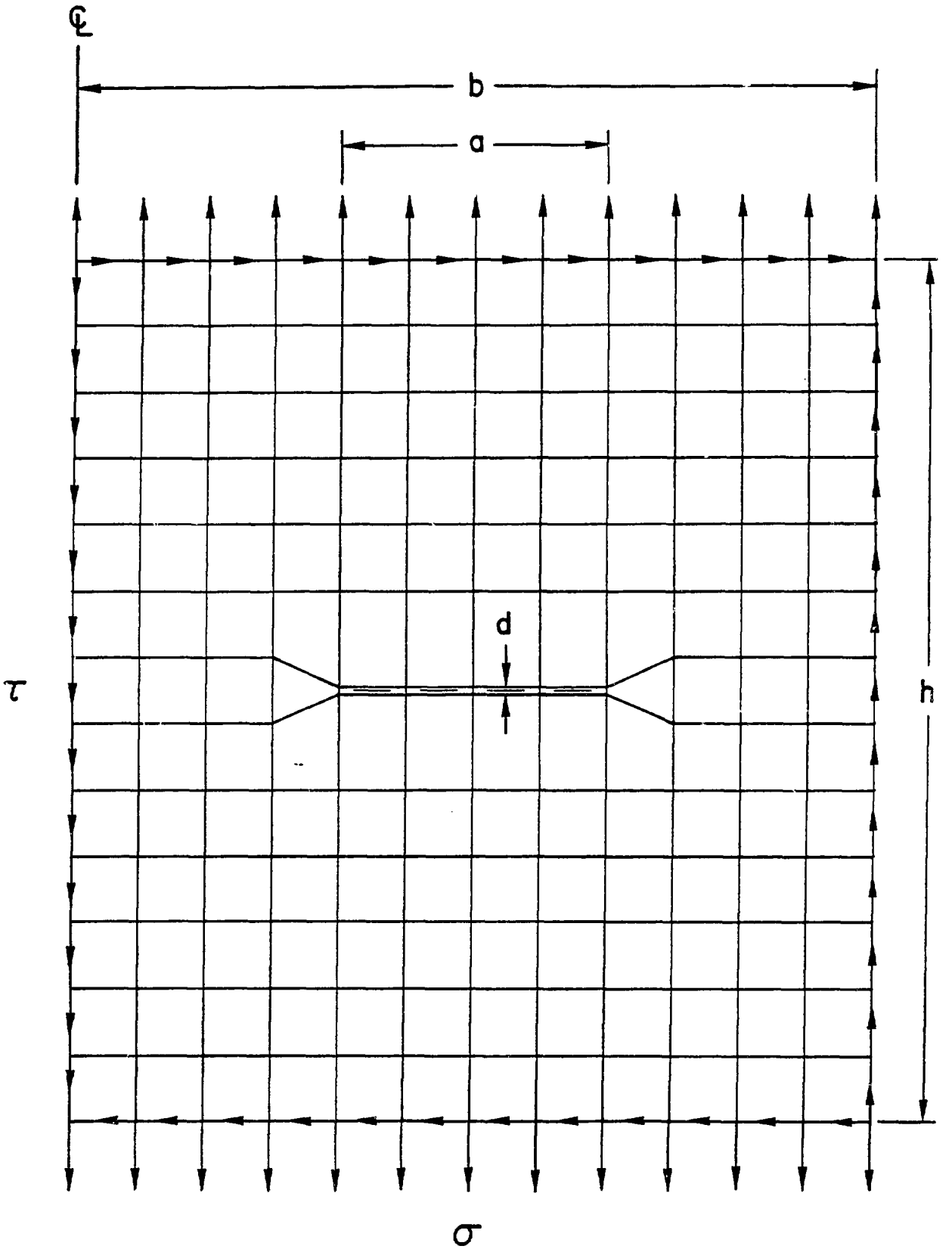

(b)

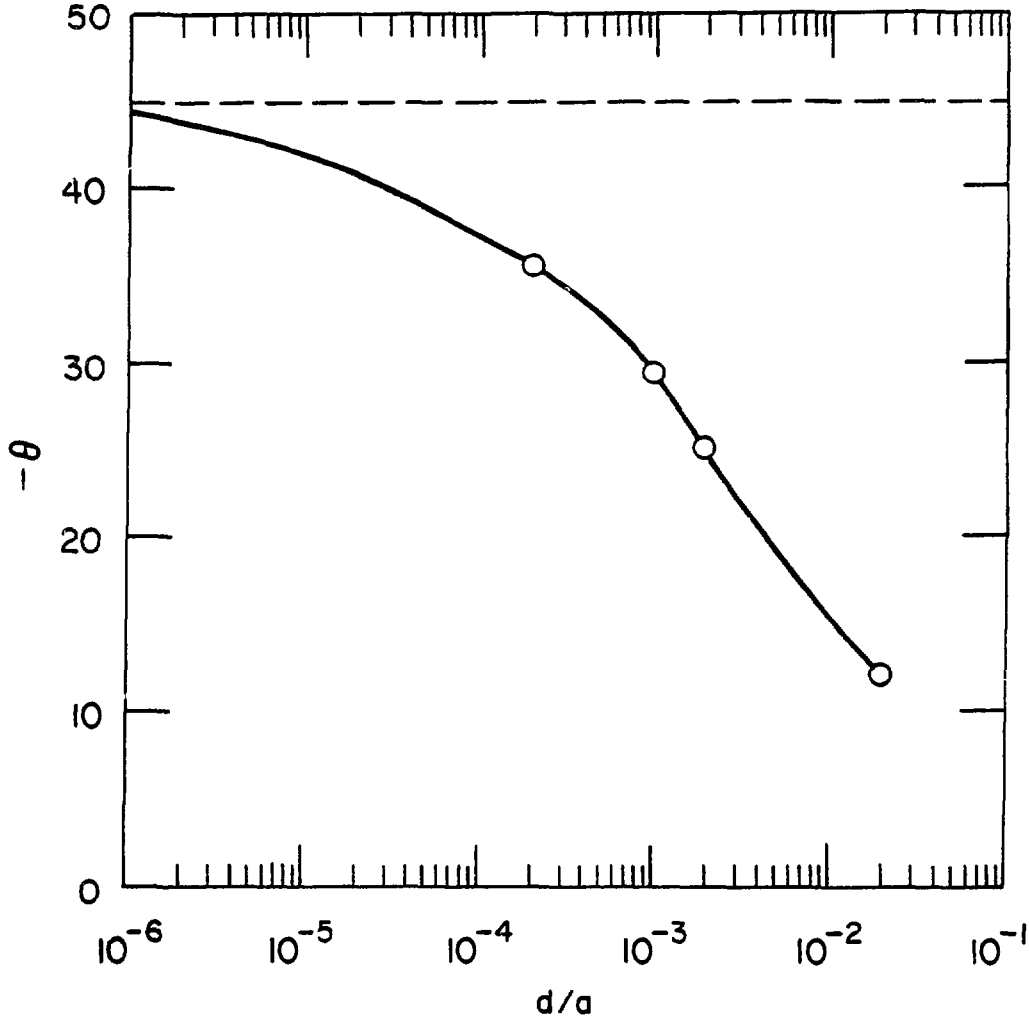
50
40
30
20
10
0
-θ
10^-6
10^-5
10^-4
10^-3
10^-2
10^-1
d/a

σ
σ